

# Vaccinia Virus-mediated Expression of Human Erythropoietin in Tumors Enhances Virotherapy and Alleviates Cancer-related Anemia in Mice

Duong H Nguyen<sup>1</sup>, Nanhai G Chen<sup>2,3</sup>, Qian Zhang<sup>2,3</sup>, Ha T Le<sup>4</sup>, Richard J Aguilar<sup>2</sup>, Yong A Yu<sup>2,3</sup>, Joseph Cappello<sup>2</sup> and Aladar A Szalay<sup>1-3</sup>

<sup>1</sup>Department of Biochemistry, Rudolph Virchow Center for Experimental Biomedicine, and Institute for Molecular Infection Biology, University of Würzburg, Würzburg, Germany; <sup>2</sup>Genelux Corporation, San Diego Science Center, San Diego, California, USA; <sup>3</sup>Department of Radiation Medicine and Applied Sciences, Rebecca & John Moores Comprehensive Cancer Center, University of California, San Diego, California, USA; <sup>4</sup>Department of Microbiology, Military Institute of Hygiene and Epidemiology, Hanoi, Vietnam

Recombinant human erythropoietin (rhEPO), a glycoprotein hormone regulating red blood cell (RBC) formation, is used for the treatment of cancer-related anemia. The effect of rhEPO on tumor growth, however, remains controversial. Here, we report the construction and characterization of the recombinant vaccinia virus (VACV) GLV-1h210, expressing hEPO. GLV-1h210 was shown to replicate in and kill A549 lung cancer cells in culture efficiently. In mice bearing A549 lung cancer xenografts, treatment with a single intravenous dose of GLV-1h210 resulted in tumor-specific production and secretion of functional hEPO, which exerted an effect on RBC progenitors and precursors in the mouse bone marrow, leading to a significant increase in the number of RBCs and in the level of hemoglobin. Furthermore, virally expressed hEPO, but not exogenously added rhEPO, enhanced virus-mediated green fluorescent protein (GFP) expression in tumors and subsequently accelerated tumor regression when compared with the treatment with the parental virus GLV-1h68 or GLV-1h209 that expressed a nonfunctional hEPO protein. Moreover, intratumorally expressed hEPO caused enlarged tumoral microvessels, likely facilitating virus spreading. Taken together, VACV-mediated intratumorally expressed hEPO not only enhanced oncolytic virotherapy but also simultaneously alleviated cancer-related anemia.

Received 24 December 2012; accepted 9 June 2013; advance online publication 2 July 2013. doi:10.1038/mt.2013.149

## INTRODUCTION

New therapies using oncolytic viruses are emerging as promising treatment options for many types of cancer. GLV-1h68 is a genetically engineered, attenuated vaccinia virus (VACV) derived from the LIVP strain.<sup>1</sup> In preclinical models, GLV-1h68 was effective in treating many types of cancer such as human breast carcinoma,<sup>1</sup> pleural mesothelioma,<sup>2</sup> pancreatic carcinoma,<sup>3</sup> squamous

carcinoma,<sup>4</sup> melanoma lymph node metastasis,<sup>5</sup> and human primary prostate carcinoma and metastasis.<sup>6</sup> In recent times, the first phase I clinical trial with GLV-1h68 (the clinical version of GLV-1h68) in patients with advanced solid tumors was completed, demonstrating initial evidence of antitumor activity without toxicity concerns.<sup>7</sup>

Cancer-related anemia either as a primary consequence of tumor burden or secondary to aggressive radio- or chemotherapy is prevalent in cancer patients.<sup>8</sup> Anemia negatively affects normal mental and physical functions with common symptoms such as fatigue, headache, and depression.<sup>9</sup> In addition, severe anemia can limit the duration and dose of chemotherapy that a patient can endure. Recombinant human erythropoietin (rhEPO), a glycoprotein hormone regulating red blood cell (RBC) formation, is approved for the treatment of cancer-related anemia. It has shown benefits in correcting anemia and subsequently improving health-related quality of life<sup>8,10,11</sup> or enhancing radio- and chemotherapy.<sup>12,13</sup> However, the data of several clinical trials have suggested that rhEPO may promote tumor growth, which has raised questions concerning the safety of using rhEPO during cancer treatment.<sup>14,15</sup> In some animal experiments, rhEPO appeared to have antiapoptotic effects,<sup>16</sup> induced angiogenesis, and promoted tumor growth<sup>17</sup> while in others, such effects were not observed.<sup>18-20</sup> The effects of hEPO treatment in tumor models remain controversial and need further investigation.

In this study, we constructed and characterized hEPO-expressing VACVs (EPO-VACVs) and investigated the effects of hEPO expressed locally in tumors. Effects on virus replication, tumor regression, blood cell production, and tumor vascularization as well as immune cell infiltration were evaluated.

## RESULTS

### Construction of EPO-VACVs

GLV-1h209 and GLV-1h210 (Figure 1a) were derived from the genetically modified and attenuated VACV, GLV-1h68. This parental virus has three foreign gene expression cassettes, the *Renilla* luciferase-*Aequorea* green fluorescent protein (GFP)

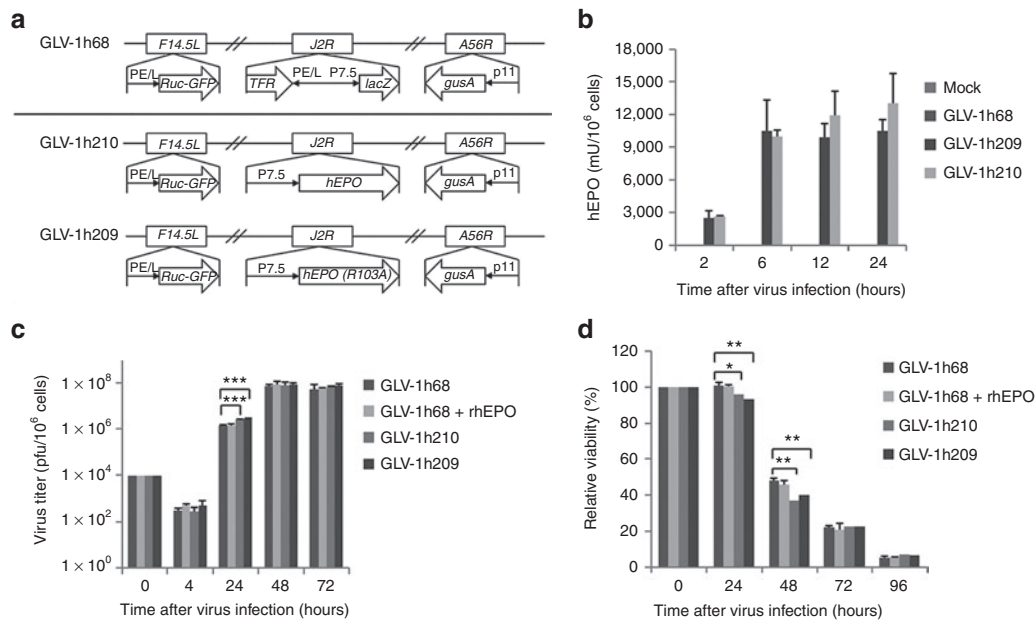


**Figure 1** Efficient replication and cytolysis of hEPO-expressing VACVs in the A549 lung cancer cell culture. **(a)** Schematic representation of GLV-1h209 and GLV-1h210 constructs. All EPO-VACV constructs were derived from the parental virus GLV-1h68. The  $\beta$ -galactosidase expression cassette in GLV-1h68 was replaced with the hEPO expression cassette or the hEPO (R103A) mutant expression cassette under the control of the vaccinia 7.5-K early promoter P7.5E to yield GLV-1h210 and GLV-1h209, respectively. Ruc-GFP is the *Renilla* luciferase-*Aequorea* GFP fusion protein. PE/L, P11, and P7.5 are VACV synthetic early/late, 11-K late, and 7.5-K early/late promoters, respectively. Tfr is the human transferrin receptor inserted in the reverse orientation with respect to the promoter PE/L. **(b)** Quantification of secreted hEPO protein in the supernatants from cells infected with different EPO-VACVs at an MOI of 10 at 2, 6, 12, and 24 hpi ( $n = 3$ ). **(c)** Virus replication curves of different EPO-VACVs. A549 cells in 24-well plates were infected with GLV-1h68, GLV-1h68 in the presence of rhEPO (epoetin alfa, 10 U/ml), GLV-1h209, or GLV-1h210 at an MOI of 0.01 in triplicate. Cells and supernatants were collected at 4, 24, 48, and 72 hpi for virus titration using plaque assays in CV-1 cells. Significant differences were shown between GLV-1h68 and GLV-1h210 or GLV-1h68 and GLV-1h209. **(d)** Cytotoxicity of different EPO-VACVs. Cells were prepared and infected as in **c**. Cell viability was measured every day for 4 consecutive days using the MTT assay. Data are shown as percentage of viability of virus-infected cells over uninfected controls. Uninfected cells at each timepoint were considered as 100% viability. Data are presented as average values with SD. \* $P < 0.05$ ; \*\* $P < 0.01$ ; \*\*\* $P < 0.001$ . GFP, green fluorescent protein; hpi, hour post-injection; MOI, multiplicity of infection; rhEPO, recombinant human erythropoietin; VACV, vaccinia virus.

fusion protein (Ruc-GFP),  $\beta$ -galactosidase and  $\beta$ -glucuronidase, inserted into the genome of the LIVP strain.<sup>1</sup> In GLV-1h209 and GLV-1h210, the  $\beta$ -galactosidase expression cassette was replaced with the hEPO expression cassette containing the vaccinia early promoter P7.5E. In GLV-1h209, a single base substitution in the cDNA-encoding hEPO resulted in the replacement of arginine with alanine at the amino acid position 103 (R103A). This substitution results in complete loss of hEPO bioactivity.<sup>21</sup> The expression of Ruc-GFP and  $\beta$ -glucuronidase in GLV-1h209 and GLV-1h210 remained intact (**Supplementary Figure S1**).

### Quantification of virally expressed hEPO in cell culture

hEPO expression from EPO-VACV-infected A549 cells was quantified by ELISA using two nonoverlapping monoclonal anti-hEPO antibodies at multiple timepoints post-infection. This assay detects hEPO protein independently of its activity. The expression of hEPO was clearly demonstrated in GLV-1h210- and GLV-1h209-infected cells (**Figure 1b**). At a multiplicity of infection of 10, hEPO protein levels increased from 2 to 6 hours post-injection (hpi), at which time all A549 cells appeared to be infected, and no further increase was found in hEPO protein expression at 12 or 24 hpi. No hEPO was detected in mock or GLV-1h68-infected cells.

### hEPO does not have a negative effect on virus replication and virus-mediated cytolysis in cell culture

The effect of hEPO on VACV replication and its cytolytic activity was evaluated in A549 cells that were infected either with GLV-1h68 in the presence or absence of rhEPO added to the media, or with GLV-1h209 (expressing nonfunctional hEPO) or GLV-1h210 (expressing functional hEPO), all at a multiplicity of infection of 0.01. Virus replication was significantly higher for GLV-1h209 and GLV-1h210 compared with GLV-1h68 or GLV-1h68 plus rhEPO at 24 hpi (**Figure 1c**), although there was no difference at later timepoints (48 and 72 hpi). As expected, cell viability showed an inverse relationship with virus replication (**Figure 1d**). At 24 and 48 hpi, slightly more cells were killed in GLV-1h209- or GLV-1h210-infected cells in comparison with GLV-1h68-infected cells in the presence or absence of rhEPO. For all viruses, cell death increased significantly at 48 hpi (more than 50% cell death), and at 96 hpi, more than 92% of cells were dead in all virus-infected cultures. No differences in virus replication and cytotoxicity between GLV-1h209 and GLV-1h210 were noted. Exogenously added rhEPO did not affect GLV-1h68 replication and its cytotoxicity. In addition, GLV-1h213, a similar viral construct that expresses functional hEPO under the control of the VACV strong synthetic late promoter (**Supplementary Figure S2a**) showed a similar virus replication to GLV-1h68 (**Supplementary Figure S2b**). Therefore,

whether virally expressed or added to media, hEPO did not interfere with virus replication and cytolysis.

### Intratumorally expressed hEPO enhances VACV-mediated GFP expression in tumors

The *in vivo* replication and distribution of EPO-VACVs was evaluated in tumor-bearing mice treated with GLV-1h210, GLV-1h68, or GLV-1h209 at 14 days post-infection (dpi). Tumor, brain, lungs, liver, heart, kidneys, spleen, and blood were harvested, examined, and tested for virus distribution (**Supplementary Table S1**). Small or negligible amounts of virus were found in the lungs, spleen, kidneys, or heart in some of the GLV-1h68-, GLV-1h209-, or GLV-1h210-treated mice, but no virus was detected in the brain, liver, or serum. In contrast, very high titers, ranging from  $10^6$  to  $10^7$  plaque-forming units/g tissue, were recovered from tumors of all infected mice. The virus titer in tumors from GLV-1h210-treated mice was higher than that from GLV-1h68-treated ( $P = 0.016$ ) and GLV-1h209-treated ( $P = 0.25$ ) mice. The difference in the virus titer between GLV-1h210 and GLV-1h209 was not statistically significant, probably owing to the limited number of tumors ( $n = 4$ ) used for viral titer analysis. The GFP signal

intensity of GLV-1h210-treated tumors (15 sections, three sections per tumor), however, was significantly higher than that of GLV-1h209-treated tumors ( $P = 0.016$ ) (**Figure 2a**). The GFP signals in treated mice were also monitored noninvasively. During the first 2 weeks after virus treatment, stronger GFP signals from tumors colonized with GLV-1h210 were noticed in comparison with tumors colonized with GLV-1h209 or GLV-1h68 (**Figure 2b**). GFP signals decreased as tumors shrank. No GFP or luciferase signals were seen in healthy organs. Furthermore, the GLV-1h213 viral titer in tumors was 3.5 times as high as the GLV-1h68 titer ( $P = 0.0014$ , **Supplementary Figure S2c**) although GLV-1h213 showed a similar virus replication to GLV-1h68 in culture. Thus, intratumorally expressed functional hEPO indeed enhanced VACV replication in tumors.

### VACV-mediated intratumorally expressed hEPO enhances tumor regression

Mice-bearing A549 tumor xenografts were treated with the parental virus GLV-1h68, GLV-1h210 expressing functional hEPO, GLV-1h68 coadministered with rhEPO, rhEPO alone, or were untreated (**Figure 3a**). Treatment with rhEPO (nine consecutive days, 500 U/kg) by itself did not result in any differences in tumor volume when compared with untreated controls. Animals of both groups had to be killed at day 35 due to excessive tumor burden. GLV-1h68 yielded reduced tumor volumes beginning at about day 28 compared with untreated controls and tumor regression

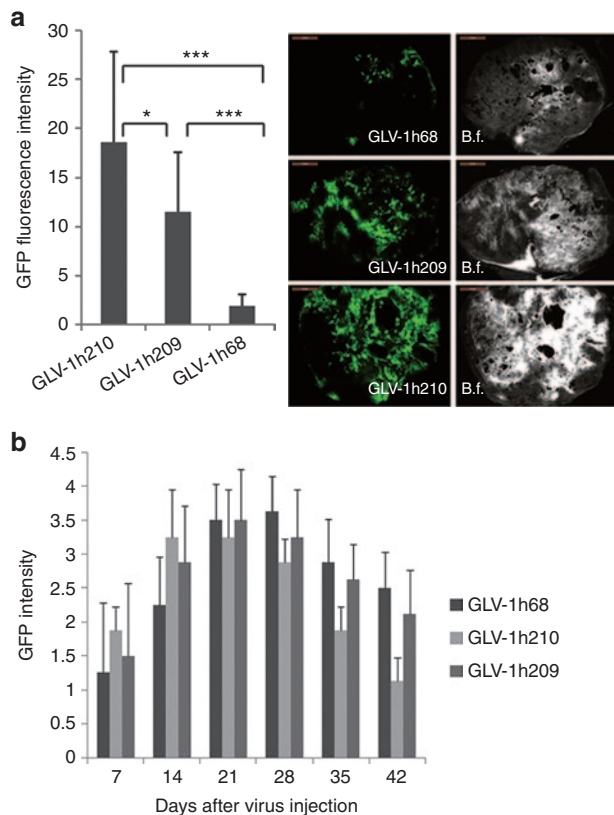


**Figure 2** GFP signal intensity in tumors. Tumor-bearing mice were injected with  $5 \times 10^6$  pfu of GLV-1h210, GLV-1h209, and GLV-1h68 or no treatment. At 14 dpi, five tumors in each group were excised and sectioned as 100  $\mu$ m slices. **(a)** Average GFP signal intensity of 15 sections was measured using ImageJ software (three sections per tumor). A representative GFP signal in each group is shown with the scale bars of 2 mm. B.f., bright field. **(b)** Kinetic changes of GFP signals in tumors treated with GLV-1h68, GLV-1h209, and GLV-1h210 measured weekly. \* $P < 0.05$ ; \*\*\* $P < 0.001$ . GFP signal intensity was scored on a 4-point system after virus treatment. dpi, day post-infection; GFP, green fluorescent protein; pfu, plaque-forming unit.

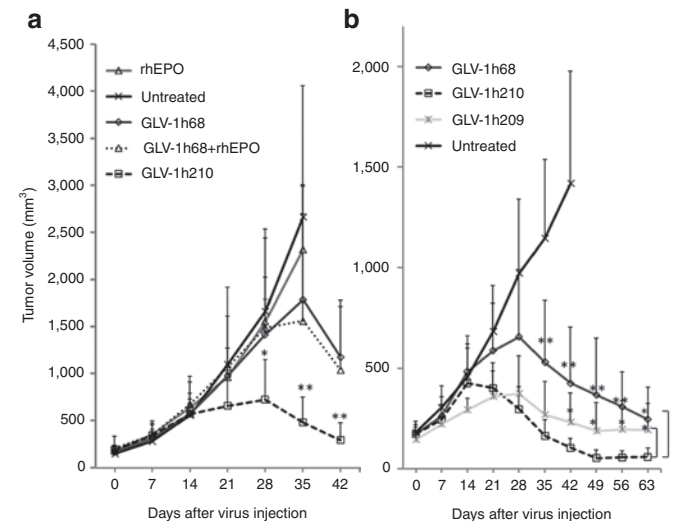


**Figure 3** Tumor regression after treatment with **(a)** GLV-1h210, GLV-1h68, GLV-1h68 plus rhEPO or rhEPO alone, or **(b)** GLV-1h210, GLV-1h209, GLV-1h68. Five to six weeks old male athymic nude mice were implanted subcutaneously with  $5 \times 10^6$  A549 cells on the right-hand flank. About 3 weeks later, tumor-bearing mice were r.o. injected with a single dose of  $2 \times 10^6$  pfu/mouse. Concomitantly, 500U/kg of rhEPO was subcutaneously injected into the rhEPO group or GLV-1h68 combined with rhEPO group for nine consecutive days after virus injection (days 1–9). Tumor volumes were measured every week. Data showed as average values with SD of six mice (in **a**) and eight mice (in **b**) in each group. Asterisks indicate significant differences of GLV-1h210 compared with GLV-1h68 (as shown in **a**), and GLV-1h210 compared with GLV-1h68 (upper asterisks) or GLV-1h209 (lower asterisks) (as shown in **b**). \* $P < 0.05$ ; \*\* $P < 0.01$ . rhEPO, recombinant human erythropoietin; r.o., retro-orbitally.

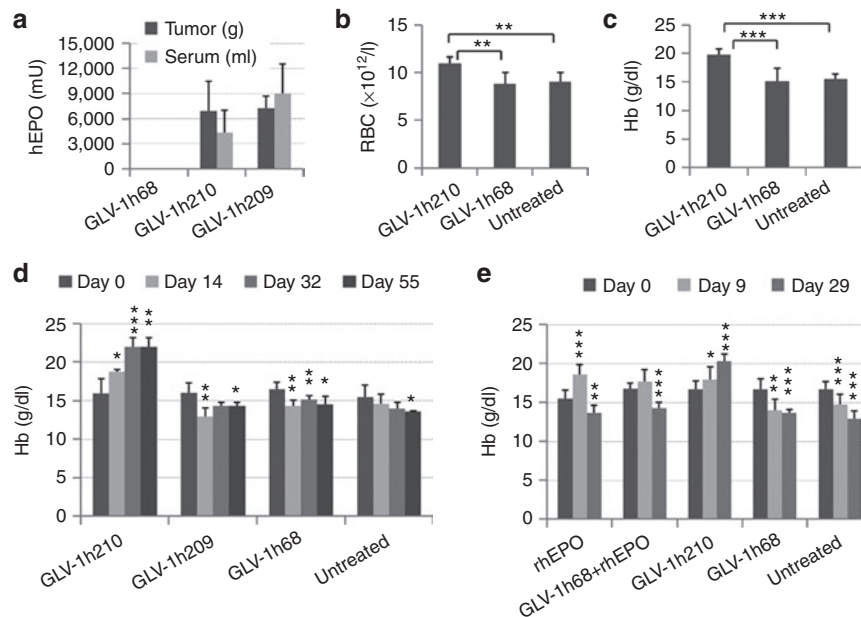


**Figure 4** The effects of virally expressed hEPO on blood cell populations. Tumor-bearing mice were injected r.o. with a single dose of  $2 \times 10^6$  pfu of GLV-1h210, GLV-1h68, or GLV-1h209. **(a)** At 14 dpi, four mice in each group were euthanized and hEPO protein in tumors and sera were tested by ELISA; 0.1 ml of whole blood was taken r.o. from each mouse for **(b)** RBCs and **(c)** Hb tests. **(d)** Time course assessment of Hb levels ( $n = 4-5$ ). **(e)** Tumor-bearing mice were treated with  $2 \times 10^6$  pfu of GLV-1h210, GLV-1h68. Concomitantly, 500 U/kg rhEPO was injected subcutaneously for nine consecutive days after virus injection (days 1–9) into the rhEPO and rhEPO + GLV-1h68 groups. Hb levels were measured at day 0, day 9, and day 29 after virus injection ( $n = 7-10$ ). Significant differences were determined between day 0 and later timepoints. \* $P < 0.05$ ; \*\* $P < 0.01$ ; \*\*\* $P < 0.001$ . dpi, day post-infection; Hb, hemoglobin; pfu, plaque-forming unit; rhEPO, recombinant human erythropoietin; r.o., retro-orbitally.

occurred after day 35. GLV-1h68 plus rhEPO (nine consecutive days, 500 U/kg) was no more effective than GLV-1h68 alone. Treatment with GLV-1h210, however, resulted in significantly greater tumor shrinkage than treatment with GLV-1h68 or with GLV-1h68 plus rhEPO. Reduced tumor size was apparent after day 14 and tumor regression began at day 28.

In a separate study (**Supplementary Figure S3**), rhEPO was injected thrice per week until the termination of the experiment (42 dpi) to investigate the effect of timing, dosing, or duration of rhEPO administration. Under all conditions, GLV-1h68 and rhEPO treatment did not show any statistically significant differences in tumor growth as compared with GLV-1h68 treatment alone. This was true irrespective of the start time of rhEPO treatment (initiated 1 week before, at the same time, or 1 week after GLV-1h68 administration) or the dose administered (high dose, EPO-H, 1,000 U/kg or low dose, EPO-L, 100 U/kg).

In another experiment, we tested whether the bioactivity of functional hEPO was required for the enhanced therapeutic effect seen for GLV-1h210. Mice-bearing A549 tumor xenografts were treated with the parental virus GLV-1h68, GLV-1h209 expressing nonfunctional mutant hEPO, and GLV-1h210 expressing functional hEPO or untreated (**Figure 3b**). GLV-1h210-treated mice exhibited overall greater tumor regression than GLV-1h68- or GLV-1h209-treated mice, while GLV-1h209 showed greater tumor regression than GLV-1h68. The tumor regression for GLV-1h210-treated mice started at day 14, whereas tumor regression began at day 28 for GLV-1h68- and GLV-1h209-treated mice. After day 28, GLV-1h210 treatment resulted in the smallest tumors, and at day 42, the difference in the tumor volume between

GLV-1h210- and GLV-1h209-treated mice was statistically significant. In untreated control mice, tumors showed continuous growth, and all mice had to be killed due to tumor burden before the experiment was terminated. In addition, GLV-1h213-treated tumors showed accelerated regression compared with tumors treated with GLV-1h68 (**Supplementary Figure S2d**).

#### Intratumorally expressed hEPO or exogenously added rhEPO results in an increase in the number of RBCs and in the level of hemoglobin

The hematological effects of virally expressed hEPO in tumors was evaluated in A549 tumor-bearing mice treated with GLV-1h210, GLV-1h209, or GLV-1h68. At 14 dpi, hEPO protein expression was detected in tumors and sera from GLV-1h210- and GLV-1h209-treated mice (**Figure 4a**). Whole blood samples were collected and evaluated for blood cell counts and hemoglobin (Hb) levels. The virally expressed hEPO from GLV-1h210 stimulated RBC production (**Figure 4b**) and increased Hb levels (**Figure 4c**), but did not cause any changes in the size of RBCs (**Supplementary Figure S4a**) nor their Hb content (**Supplementary Figure S4b**). hEPO had no effect on the total number of white blood cells (**Supplementary Figure S4c**) or individual numbers of lymphocytes, monocytes, neutrophils, or platelets (**Supplementary Figure S4d**). Although GLV-1h209-treated mice showed expression of hEPO protein in tumors and sera, there was no effect on Hb levels (**Figure 4d**), confirming that the hEPO expressed from GLV-1h209 was not biologically active. In addition, compared with the levels of Hb before treatment, a single treatment with GLV-1h210 increased and maintained Hb levels throughout the experimental period

(day 55), while untreated mice or mice treated with GLV-1h68 or GLV-1h209 showed a decline (Figure 4d). In another experiment, treatment with rhEPO daily for 9 days alone or in combination with GLV-1h68 increased Hb levels at day 9. However, after the treatment stopped, Hb levels declined below pretreatment levels (Figure 4e). These results demonstrated that hEPO expressed by GLV-1h210 increased Hb levels in tumor-bearing mice, alleviating tumor-related anemia. Moreover, the effect was sustained throughout the experiment after only a single administration of GLV-1h210. Interestingly, in some GLV-1h210-treated animals in which tumors were completely eradicated, Hb levels returned to normal baseline at day 90 after virus injection (Supplementary Table S2).

### Intratumorally expressed hEPO causes enlarged tumoral micro-blood vessels

Optical imaging and histological staining clearly demonstrated the extent of infection of tumors with GLV-1h68 or GLV-1h210, and the coincident expression of hEPO in the latter (Figure 5). At 28 dpi, the infection of the tumors resulted in notable tissue changes including massive cell death as shown by hematoxylin and eosin staining. In particular, GLV-1h210-treated tumors appeared to have larger tumor blood vessels. To investigate this effect, A549 tumor-bearing mice were treated retro-orbitally either with GLV-1h210, GLV-1h209, or GLV-1h68 at a dose of  $5 \times 10^6$  plaque-forming units. At 14 dpi, five animals from each group were killed. Tumors were excised and processed with agarose-embedded sectioning and stained for the blood vessel marker CD31 (Figure 6). The results revealed that while the mean blood vessel diameter of all virally infected tumors were greater than the untreated controls, the highest mean blood vessel diameter was observed in the GLV-1h210-treated tumors, which was statistically significant over all other groups ( $P < 0.001$ ). Importantly, treatment with virus did not affect the number of blood vessels in tumors. The mean blood vessel density in all virally treated groups was not different from the untreated controls.

### Intratumorally expressed hEPO does not affect the innate immune response in nude mice

While our results showed that hEPO expression did not affect white blood cell counts in circulation, it was possible that the population of immune cells within the tumor was altered. Tumors at 14 dpi were stained for major histocompatibility complex-II-positive cells (B cells, macrophages, and dendritic cells) (Figure 7). GLV-1h210- and GLV-1h209-treated tumors showed significantly higher positive staining compared with GLV-1h68 treated or untreated controls, indicating enhanced immune recruitment into GLV-1h210- or GLV-1h209-treated tumors. This enhanced immune recruitment was most likely due to enhanced virus replication of GLV-1h209 and GLV-1h210 in tumors when compared with GLV-1h68. Consistent with the higher viral titer of GLV-1h210 in tumors than GLV-1h209, the average value of major histocompatibility complex-II fluorescent intensity of GLV-1h210-treated tumors was higher than that of the GLV-1h209 group, although the difference was not statistically significant. In addition, the expression of 58 immune-related antigens in tumors was analyzed (Supplementary Table S3). No differences between GLV-1h210

and GLV-1h209 (ratio  $>2$  or  $<0.5$ ) were seen. Thus, the expression of functional hEPO in tumors had no immune modulation effect in the immuno-compromised nude-mouse model.

## DISCUSSION

GLV-1h68 has been successfully used to treat many types of cancer in various preclinical models. It can be used as a monotherapy<sup>1,2,6,22</sup> or can be combined with chemotherapy<sup>23</sup> or radiotherapy.<sup>24</sup> Moreover, transgenes in VACV were shown to improve

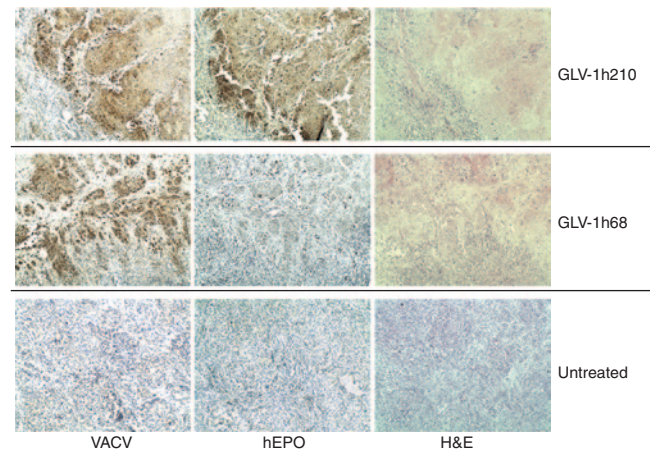


**Figure 5** Optical and histological analyses of VACV-infected tumor xenografts. Tumor-bearing mice were injected with a single dose of  $2 \times 10^6$  pfu of GLV-1h210, GLV-1h68. At 28 dpi, tumors were excised and processed for paraffin-embedded sectioning. Adjacent  $5 \mu\text{m}$  sections were stained either with anti-VACV, anti-hEPO antibodies or H&E. Hematoxylin counterstaining was used for the background separation. Images were captured at  $\times 100$  original magnification. Furthermore, left pictures are *Renilla-luciferase* (Ruc) and green fluorescent protein (GFP) encoded by VACVs, which were imaged before tumors were excised. dpi, day post-infection; hEPO, human erythropoietin; H&E, hematoxylin and eosin; pfu, plaque-forming unit; VACV, vaccinia virus.

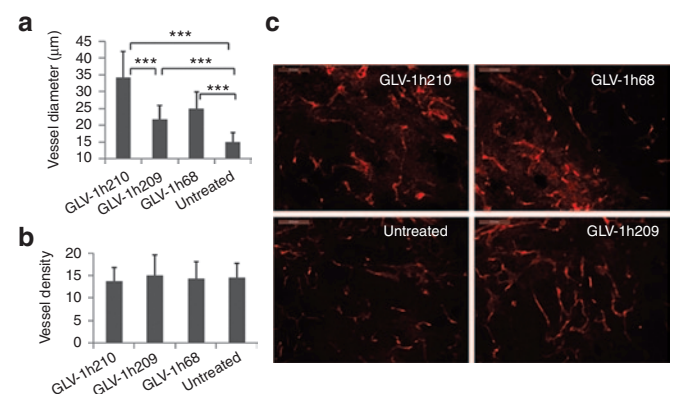


**Figure 6** The effect of virally expressed hEPO on tumor blood vessels. Tumor-bearing mice were injected with  $5 \times 10^6$  pfu of GLV-1h210, GLV-1h209, and GLV-1h68. Tumors were excised at 14 dpi and processed for agarose-embedded sectioning.  $100 \mu\text{m}$  sections were stained for blood vessels using anti-CD31 antibodies. (a) Vessel diameter and (b) density were measured. Vessel diameter and density were measured in 30 different fields of  $1.91 \times 1.43 \text{ mm}$  (two fields for one section, three sections for one tumor, and five tumors for each group) using ImageJ software. (c) A representative CD31-staining field for each group with bars of  $0.3 \text{ mm}$ .  $***P < 0.001$ . dpi, day post-infection; hEPO, human erythropoietin; pfu, plaque-forming unit.

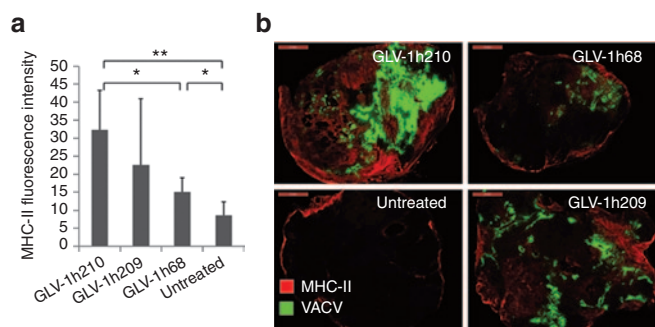


**Figure 7** Immune cell infiltration in virus-infected tumors. Tumor-bearing mice were injected with  $5 \times 10^6$  pfu of GLV-1h210, GLV-1h209, and GLV-1h68. At 14 dpi, tumors were excised and stained for MHC-II-positive cells. **(a)** Average fluorescent intensity of five tumors in each group (one section for one tumor). **(b)** A representative MHC-II-staining section in each group overlaid with the GFP signal image as an indication of VACV infection with the bars of 2 mm. \* $P < 0.05$ ; \*\* $P < 0.01$ . dpi, day post-infection; GFP, green fluorescent protein; MHC, major histocompatibility complex; pfu, plaque-forming unit; VACV, vaccinia virus.

tumor regression<sup>25</sup> and enable deep tissue imaging.<sup>26</sup> In this study, we demonstrate that the GLV-1h68-based oncolytic virotherapy platform can be engineered to express hEPO in human lung tumor xenografts in nude mice. The virally expressed hEPO increased RBC biogenesis, enlarged tumoral micro-blood vessels, and enhanced oncolytic virotherapy.

Modification of the parental virus GLV-1h68 by insertion of a hEPO expression cassette, either functional (GLV-1h210) or non-functional (GLV-1h209), enhanced viral replication of the resulting viruses in cell culture. This was due to the replacement of the VACV promoters in the parental virus (P7.5 and PE/L) with the weaker promoter, P7.5E, as we previously showed that virus replication efficiency was inversely proportionate to the transcription/translation burden added to the viral genome.<sup>27</sup> The enhanced virus replication was not due to the virally expressed hEPO since exogenously added rhEPO had no effect on GLV-1h68 replication and GLV-1h213 that expresses functional hEPO under the control of the VACV synthetic late promoter PL (the promoter PL is much stronger than the VACV 7.5K early promoter P7.5E in GLV-210 and GLV-1h209) showed almost identical replication efficiency to GLV-1h68 in cell culture. Interestingly, the GFP signal intensity in tumors treated with GLV-1h210 was significantly higher than that in tumors treated with GLV-1h209, which expresses a nonfunctional hEPO, although both GLV-1h210 and GLV-1h209 have the same promoter (P7.5E) and both showed almost identical replication efficiencies in cell culture. In addition, GLV-1h213 showed a significantly higher replication efficiency in tumors than GLV-1h68. Thus, the functional hEPO expressed from VACV enhanced VACV replication in tumors, but not in cell culture, likely by mechanisms related to physiological changes in the tumor microenvironment. By contrast, exogenously added rhEPO did not have an effect on virus replication in tumors (**Supplementary Figure S5**), probably owing to an inability of achieving and maintaining high concentrations of rhEPO in tumors after rhEPO administration. Indeed, we were not able to find any detectable amount of rhEPO in both tumors and sera at 1 day after rhEPO administration despite the different doses and intervals of rhEPO administration that we tested.

During evaluation of GLV-1h213 in mice (**Supplementary Figure S2**), we noticed GLV-1h213 toxicity was enhanced in mice in comparison with GLV-1h68 and GLV-1h210. Therefore, the toxicity of GLV-213 did not allow extensive comparison with GLV-1h68. We also constructed an additional hEPO-expressing VACV (GLV-1h211). GLV-1h211 is identical to GLV-1h213 and GLV-1h210 structurally, but EPO expression is driven by the VACV synthetic early promoter (PE) that is weaker than the PL promoter in GLV-1h213, but is stronger than the P7.5E promoter driving EPO expression in GLV-1h210. Surprisingly, GLV-1h211 with EPO expression from the PE promoter was still toxic to mice compared with GLV-1h68 and GLV-1h210. It is evident that high-level overexpression of hEPO in tumors is toxic to mice. We found that the level of hEPO expression mediated by GLV-1h210 was optimal since no overt toxicity was observed in mice.

One important factor contributing to tumor growth is angiogenesis. Here, we show that VACV-mediated expression of hEPO in tumors did not affect tumor microvessel density. However, bigger blood vessels were observed in the VACV-treated tumors compared with untreated controls ( $P < 0.001$ ). Enlargement of tumoral blood vessels after VACV tumor infection has been previously reported.<sup>28</sup> Furthermore, the vessel enlargement was more prominent in GLV-1h210-treated tumors compared with GLV-1h209 ( $P < 0.001$ ) or GLV-1h68 ( $P < 0.001$ ). The results suggest that functional hEPO modulates the tumor microenvironment, leading to enlarged micro-blood vessels without promoting tumor neoangiogenesis. Vessel dilatation was shown to increase vascular permeability, thus, facilitating virus spreading locally.<sup>29</sup> The administration of hEPO has been shown to increase vascular permeability enhancing chemotherapy with 5-fluorouracil without neoangiogenic effects.<sup>30</sup> Our results suggest that hEPO expressed from GLV-1h210 further enhanced tumoral microvessel enlargement without an increase in the number of blood vessels.

Administration of rhEPO has been reported to increase levels of endogenous polyclonal immunoglobulins, B cells,<sup>31</sup> T cells,<sup>32</sup> and/or dendritic cells.<sup>33</sup> These immune cells play an important role in controlling tumor growth and rejection.<sup>34,35</sup> In this study, we did not see any effects of functional hEPO on immune cell infiltration and cytokine/chemokine expression in tumors. The degree of immune infiltration and cytokine/chemokine expression was directly correlated to the number of virus particles detected in the tumor tissue,<sup>3,22,28</sup> supporting the simple conclusion that higher virus titers recruit more immune cells and elicit greater secreted cytokines/chemokines. It is noteworthy that in these studies we used T cell-deficient nude mice, which are not an ideal model for evaluation of the innate immune response.

rhEPO was approved for the treatment of cancer-related anemia in 1993. Clinically, it has demonstrated enormous benefits in correcting anemia that affects 90% of cancer patients, 60% of which need blood transfusion during or after cancer treatment.<sup>36</sup> Lung cancer patients in particular have an incidence of anemia of 70.9%.<sup>37</sup> Among patients receiving chemotherapy, one third develop anemia after three cycles of chemotherapy.<sup>10</sup> Here, we have shown a significant increase in the number of RBCs and the levels of Hb following treatment with GLV-1h210, while mice treated with GLV-1h68, GLV-1h209, or untreated controls showed a decrease in the levels of Hb. In addition to erythropoiesis, EPO

has been reported to have antiapoptotic effects, which promote proliferation and migration of endothelial cells<sup>38</sup> in which the EPO receptor is highly expressed.<sup>39</sup> The antiapoptotic effect is thought to be initiated by the binding of EPO to EPO receptor, leading to the activation of Janus Kinase-2 (JAK-2), and then triggering a series of downstream cascades.<sup>40–42</sup> Some preclinical studies have suggested that treatment with rhEPO may promote angiogenesis and tumor growth,<sup>17</sup> while others showed no such effects.<sup>18,19</sup> Our results revealed that hEPO expressed from GLV-1h210 in tumors did not promote tumor growth. Rather, it enhanced the efficacy of VACV-mediated oncology.

In summary, hEPO expressed from VACV in tumors significantly increased the number of RBCs, Hb levels, virus replication in tumors, and enhanced tumor regression in the A549 lung tumor xenograft model. Locally expressed hEPO caused enlargement of tumoral microvessels, which facilitated virus spreading and tumor regression. It is conceivable that in clinical settings, the combined benefits of EPO-VACV treatment, enhanced oncolytic activity, and systemic erythropoiesis, could simultaneously improve treatment and ameliorate anemia in patients with cancer.

## MATERIALS AND METHODS

**Cell lines.** All cell lines used in this study were obtained from the American Type Culture Collection (Manassas, VA). African green monkey kidney fibroblast CV-1 cells were cultured in Dulbecco's modified Eagle's medium, supplemented with 1% antibiotic-antimycotic (AA) solution (Mediatech, Manassas, VA; 100 U/ml penicillin G, 250 ng/ml amphotericin B, 100 units/ml streptomycin) and 10% fetal bovine serum (Mediatech). Human lung cancer cell line A549 cells were cultured in RPMI 1640, supplemented with 10% fetal bovine serum and 1% AA. Cells were grown at 37 °C under 5% CO<sub>2</sub>.

**Construction of hEPO-expressing VACVs.** The cDNA-encoding hEPO was PCR-amplified with primers EPO5 (5'-GTCGAC (Sal I) CAC-CATGGGGGTGCACGAATGTCC-3') and EPO3 (5'-TTAATTAA (Pac I) TCATCTGTCCCCTGTCTGC-3') using a DNA plasmid from OriGene (Rockville, MD) as the template (cat. no. TC125341). The PCR product was gel purified and cloned into pCR-Blunt II-TOPO vector using the Zero Blunt TOPO PCR Cloning Kit (Life Technologies, Carlsbad, CA). The hEPO cDNA was then released by restriction enzyme digestion with Sal I and Pac I, and subcloned into the VACV TK-transfer vectors.<sup>27</sup> The hEPO-expressing VACV strain GLV-1h210 was constructed by amplifying the cDNA for hEPO with primers P7.5Ec-epo5 (5'-GAGCTC(SacI) AAAAGTAGAAAATATATTCTAATTTATTGCACGGTGCACCAC-CATGGGGGT-3') and SacI-epo3 (5'-TCCGAGCTC(Sac I)TCCAGACATTGTTG-3') using the hEPO-containing TK-transfer vectors described above as the template. The PCR product was cloned into pCR-Blunt II-TOPO vector, released by restriction with Sac I, and subcloned into the TK-transfer vector. The resulting construct TK-P7.5E-hEPO thus contained the hEPO cDNA under the control of vaccinia natural early promoter P7.5E and was used for construction of recombinant GLV-1h210 with GLV-1h68 as the parental virus. GLV-1h209 was generated similarly, but expressing a mutated, nonfunctional hEPO (R103A). TK-P7.5E-hEPO vector was used as the template for site-direct mutagenesis using a pair of primers (5'-GCCGTCAGTGGCCTTGCCAGCCTACCA-3' and 5'-TGGTGAGGCTGGCAAGGCCACTGACGGC-3'), resulting in arginine replaced with alanine at the amino acid position 103 of hEPO (hEPO-R103A) (Quick Change II XL site directed mutagenesis kit; Agilent technologies, Santa Clara, CA). The mutation was confirmed by DNA sequence analysis. GLV-1h209 was produced using the TK-P7.5E-hEPO-R103A transfer vector and the parental virus GLV-1h68. The recombinant viruses were selected and purified as described previously.<sup>43</sup>

**Virus replication assay.** Monolayers of A549 cells were infected with each virus at a multiplicity of infection of 0.01 for 1 hour. At 4, 24, 48, and 72 hpi, three individual-infected wells of each virus were harvested, serially diluted in Dulbecco's modified Eagle's medium with 2% fetal bovine serum and titrated in CV-1 cells in duplicate. Where indicated, rhEPO (epoetin alfa; Amgen, Thousand Oaks, CA) was added to infection and culture media and remained until time of harvest at a final concentration of 10 U/ml.

**Quantification of hEPO expression.** Tumor-bearing mice were killed at 14 days after treatment with each virus. Tumors were excised and homogenized in lysis buffer (50 mmol/l Tris-HCl, 2 mmol/l EDTA, pH 7.4) supplemented with complete protease inhibitor cocktail (Roche, Indianapolis, IN) using MagNA lyser (Roche) at a speed of 6,500 for 30 seconds. Tumor lysates underwent three cycles of freeze-thaw, sonication, and clarification by centrifugation at 10,000 rpm for 10 minute at 4 °C. Sera were collected by centrifugation of whole blood at 6,000 rpm for 5 minute after coagulation overnight at 4 °C. In cell culture, A549 cells were infected with each virus at a multiplicity of infection of 10 in triplicate. At 2, 6, 12, and 24 hpi, supernatants were harvested. hEPO protein levels in tumor lysates, sera, and cell culture supernatants were quantified using the EPO ELISA kit (STEMCELL Technologies, Vancouver, British Columbia, Canada).

**Animal model and tumor therapy with EPO-VACVs.** Mice were cared in accordance with approved protocols by the Institutional Animal Care and Use Committee of Explora Biolabs (San Diego Science Center, San Diego, CA). Tumors were generated by the subcutaneous implantation of A549 cells (5 × 10<sup>6</sup> cells) in the right-hind leg of 6–8 weeks old male nude mice (NCI/Hsd/Athymic Nude-Foxn1<sup>tm</sup>; Harlan, Placentia, CA). About 3 weeks after implantation, when tumors reached a volume of about 200 mm<sup>3</sup> (tumor volume was calculated following this formula: ((height – 5 mm) × width × length)/2), tumor-bearing mice were retro-orbitally injected with a single dose of 2 × 10<sup>6</sup> plaque-forming units/mouse (unless otherwise indicated) of EPO-VACVs, GLV-1h68, or received no treatment. Where indicated, rhEPO was administered subcutaneously for nine consecutive days in the left flank of mice at a dose of 500 U/kg. Tumor volume and animal weight were measured once a week. Animals were observed daily for any signs of toxicity. At the designated timepoints, mice were killed, and blood, tumor, and tissues (liver, lungs, kidneys, brain, and spleen) were collected. The samples were used for blood tests, histology, protein isolation, or determination of virus replication. GFP signals were monitored under ultraviolet light using a stereo fluorescence macro imaging system (Lighttools Research, Encinitas, CA). GFP signal intensity was scored with a 4-point system: 0, no GFP signal; 1, one spot; 2, 2 or 3, local spots; 3, more than 3 spots; and 4, diffuse signal.

**Hb test and total blood cell counts.** Mice were anesthetized using a combination of isoflurane and oxygen (VetEquip, Pleasanton, CA). Blood was taken by retro-orbital bleeding using EDTA-coated capillary tubes (Fisher Scientific, Pittsburgh, PA). Hb was measured by QuantiChrom hemoglobin assay (BioAssay Systems, Hayward, CA), and total blood cell count was determined within 2 hour of blood draw (Explora Biolabs, San Diego, CA).

**Immunohistochemical staining.** For paraffin-embedded sections, 5 μm sections were cut using an RM2125 microtome (Leica, Buffalo Grove, IL) and subjected to H&E staining (Vector Laboratories, Burlingame, CA). Adjacent sections were stained for hEPO and VACV. Rabbit anti-hEPO antibodies (1:100, M20; Santa Cruz Biotechnology, Dallas, TX) and goat anti-rabbit IgGs-conjugated HRP (Vector Laboratories) were used as primary and secondary antibody, respectively. Chromogenic detection was performed with DAB liquid substrate (Dako, Carpinteria, CA). The background was counterstained with hematoxylin. VACV staining was performed as described previously.<sup>25</sup> Stained slides were examined microscopically (Olympus IX71; Olympus, Center Valley, PA). For agarose-embedded sections, 100 μm sections were cut using a VT1200S microtome (Leica) and stained for major histocompatibility complex-II (I-A/I-E, 1:500; eBioscience, San Diego, CA)

or CD31 (PECAM-1, 1:200; BD Pharmingen, San Jose, CA).<sup>28</sup> Donkey anti-rat IgGs-conjugated Alexa Fluor 594 (1:500; Jackson ImmunoResearch, West Grove, PA) was used as a secondary antibody. Images were captured on a MZ16 FA stereo fluorescence microscope (Leica) equipped with a Firewire DFC/IC monochrome CCD camera.

**Measurement of fluorescence intensity.** Fluorescence intensity of sections stained for major histocompatibility complex-II–positive cells was measured using ImageJ software (<http://rsb.info.nih.gov/ij/>) based on brightness-related pixels with fluorescence intensity ranging from 0 to 255. All images were captured with the identical settings. Using ImageJ software, the whole image area (12.7 × 9.51 mm) was divided into 12 grids or fields. Between five and 11, fields were used to count fluorescent signal intensity. The signal intensity of each section was the average of the individually counted fields. The GFP signal intensity of virus-infected tumors was measured in the whole tumor section.

**Measurement of blood vessel density and vessel diameter.** Sections stained for CD31 were used for the measurement of blood vessel density and diameter. Under the fluorescent microscope, the magnification was fixed for all captured images with a dimension of 1.91 × 1.43 mm. Using the ImageJ software, five equally spaced horizontal lines were drawn on all captured images. All blood vessels that intersected with these lines were counted and measured for blood vessel density and diameter.

**Statistical analysis.** A two-tailed Student's *t*-test was used for statistical analysis. *P* values of <0.05 were considered statistically significant.

## SUPPLEMENTARY MATERIAL

**Figure S1.** Expression of marker genes from EPO-VACVs detected by fluorescence microscopy and X-gal, X-GLCA staining.

**Figure S2.** Virally expressed hEPO enhances virus replication in tumors, resulting in accelerated tumor regression.

**Figure S3.** Relative changes in tumor volume after treatment with GLV-1h68 in combination with rEPO (epoetin alfa).

**Figure S4.** The effects of virally expressed hEPO on blood cell populations.

**Figure S5.** Virus titer after treatment with GLV-1h68, GLV-1h210, and GLV-1h68 in combination with rEPO.

**Table S1.** Virus distribution in organs after treatment with GLV-1h68, GLV-1h209, and GLV-1h210.

**Table S2.** Hemoglobin levels return to normalcy in mice treated with GLV-1h210 after tumor eradication.

**Table S3.** Comparison of mouse immune-related antigens in tumors after treatment with GLV-1h210, GLV-1h209 or GLV-1h68.

## ACKNOWLEDGMENTS

We thank Terry Trevino, Melody Jing, and Johanna Langbein-Laugwitz for excellent technical assistance. This work was supported by a research grant from Genelux Corporation (R&D division, San Diego, CA), and a service grant to the University of Würzburg, Germany also funded by Genelux Corporation, San Diego, CA. D.H.N. was supported by a graduate stipend from Genelux Corporation. N.G.C., Q.Z., R.J.A., Y.A.Y., J.C., and A.A.S. are employees of Genelux Corporation and have personal financial interest in Genelux Corporation. The other authors declared no conflict of interest.

## REFERENCES

- Zhang, Q, Yu, YA, Wang, E, Chen, N, Danner, RL, Munson, PJ *et al.* (2007). Eradication of solid human breast tumors in nude mice with an intravenously injected light-emitting oncolytic vaccinia virus. *Cancer Res* **67**: 10038–10046.
- Kelly, KJ, Woo, Y, Brader, P, Yu, Z, Riedl, C, Lin, SF *et al.* (2008). Novel oncolytic agent GLV-1h68 is effective against malignant pleural mesothelioma. *Hum Gene Ther* **19**: 774–782.
- Yu, YA, Galanis, C, Woo, Y, Chen, N, Zhang, Q, Fong, Y *et al.* (2009). Regression of human pancreatic tumor xenografts in mice after a single systemic injection of recombinant vaccinia virus GLV-1h68. *Mol Cancer Ther* **8**: 141–151.
- Yu, Z, Li, S, Brader, P, Chen, N, Yu, YA, Zhang, Q *et al.* (2009). Oncolytic vaccinia therapy of squamous cell carcinoma. *Mol Cancer* **8**: 45.

- Kelly, KJ, Brader, P, Woo, Y, Li, S, Chen, N, Yu, YA *et al.* (2009). Real-time intraoperative detection of melanoma lymph node metastases using recombinant vaccinia virus GLV-1h68 in an immunocompetent animal model. *Int J Cancer* **124**: 911–918.
- Gentschev, I, Donat, U, Hofmann, E, Weibel, S, Adelfinger, M, Raab, V *et al.* (2010). Regression of human prostate tumors and metastases in nude mice following treatment with the recombinant oncolytic vaccinia virus GLV-1h68. *J Biomed Biotechnol* **2010**: 489759.
- Biondo, A, *et al.* (2011). 1258 POSTER Phase I clinical trial of a genetically modified oncolytic vaccinia virus GL-ONC1 with green fluorescent protein imaging. *Eur J Cancer* **47** (suppl. 1): S162.
- Bohlius, J, Weingart, O, Trelle, S and Engert, A (2006). Cancer-related anemia and recombinant human erythropoietin—an updated overview. *Nat Clin Pract Oncol* **3**: 152–164.
- Curt, GA, Breitbart, W, Cella, D, Groopman, JE, Horning, SJ, Itri, LM *et al.* (2000). Impact of cancer-related fatigue on the lives of patients: new findings from the Fatigue Coalition. *Oncologist* **5**: 353–360.
- Gaspy, J, Degos, L, Dicato, M and Demetri, GD (2002). Comparable efficacy of epoetin alfa for anemic cancer patients receiving platinum- and nonplatinum-based chemotherapy: a retrospective subanalysis of two large, community-based trials. *Oncologist* **7**: 126–135.
- Gaspy, JA (2009). Erythropoietin in cancer patients. *Annu Rev Med* **60**: 181–192.
- Littlewood, TJ, Bajetta, E, Nortier, JW, Vercaemmen, E and Rapoport, B; Epoetin Alfa Study Group (2001). Effects of epoetin alfa on hematologic parameters and quality of life in cancer patients receiving nonplatinum chemotherapy: results of a randomized, double-blind, placebo-controlled trial. *J Clin Oncol* **19**: 2865–2874.
- Lavey, RS and Dempsey, WH (1993). Erythropoietin increases hemoglobin in cancer patients during radiation therapy. *Int J Radiat Oncol Biol Phys* **27**: 1147–1152.
- Henke, M, Laszig, R, Rube, C, Schäfer, U, Haase, KD, Schilcher, B *et al.* (2003). Erythropoietin to treat head and neck cancer patients with anaemia undergoing radiotherapy: randomised, double-blind, placebo-controlled trial. *Lancet* **362**: 1255–1260.
- Leyland-Jones, B, Semiglazov, V, Pawlicki, M, Pienkowski, T, Tjulandin, S, Manikhas, G *et al.* (2005). Maintaining normal hemoglobin levels with epoetin alfa in mainly nonanemic patients with metastatic breast cancer receiving first-line chemotherapy: a survival study. *J Clin Oncol* **23**: 5960–5972.
- Ghezzi, P and Brines, M (2004). Erythropoietin as an antiapoptotic, tissue-protective cytokine. *Cell Death Differ* **11** (suppl. 1): S37–S44.
- Yasuda, Y, Fujita, Y, Matsuo, T, Koinuma, S, Hara, S, Tazaki, A *et al.* (2003). Erythropoietin regulates tumour growth of human malignancies. *Carcinogenesis* **24**: 1021–1029.
- Hardee, ME, Kirkpatrick, JP, Shan, S, Snyder, SA, Vujaskovic, Z, Rabbani, ZN *et al.* (2005). Human recombinant erythropoietin (rEpo) has no effect on tumour growth or angiogenesis. *Br J Cancer* **93**: 1350–1355.
- LaMontagne, KR, Butler, J, Marshall, DJ, Tullai, J, Gechtman, Z, Hall, C *et al.* (2006). Recombinant epoetins do not stimulate tumor growth in erythropoietin receptor-positive breast carcinoma models. *Mol Cancer Ther* **5**: 347–355.
- Swift, S, Ellison, AR, Kassner, P, McCaffery, I, Rossi, J, Sinclair, AM *et al.* (2010). Absence of functional EpoR expression in human tumor cell lines. *Blood* **115**: 4254–4263.
- Boissel, JP and Bunn, HF (1990). Erythropoietin structure-function relationships. *Prog Clin Biol Res* **352**: 227–232.
- Gentschev, I, Ehrig, K, Donat, U, Hess, M, Rudolph, S, Chen, N *et al.* (2010). Significant growth inhibition of canine mammary carcinoma xenografts following treatment with oncolytic vaccinia virus GLV-1h68. *J Oncol* **2010**: 736907.
- Sturm, JB, Hess, M, Weibel, S, Chen, NG, Yu, YA, Zhang, Q *et al.* (2012). Functional hyper-IL-6 from vaccinia virus-colonized tumors triggers platelet formation and helps to alleviate toxicity of mitomycin C enhanced virus therapy. *J Transl Med* **10**: 9.
- Advani, SJ, Buckel, L, Chen, NG, Scanderbeg, DJ, Geissinger, U, Zhang, Q *et al.* (2012). Preferential replication of systemically delivered oncolytic vaccinia virus in focally irradiated glioma xenografts. *Clin Cancer Res* **18**: 2579–2590.
- Frentzen, A, Yu, YA, Chen, N, Zhang, Q, Weibel, S, Raab, V *et al.* (2009). Anti-VEGF single-chain antibody GLAF-1 encoded by oncolytic vaccinia virus significantly enhances antitumor therapy. *Proc Natl Acad Sci USA* **106**: 12915–12920.
- Haddad, D, Chen, N, Zhang, Q, Chen, CH, Yu, YA, Gonzalez, L *et al.* (2012). A novel genetically modified oncolytic vaccinia virus in experimental models is effective against a wide range of human cancers. *Ann Surg Oncol* **19** (suppl. 3): S665–S674.
- Chen, NG, Yu, YA, Zhang, Q and Szalay, AA (2011). Replication efficiency of oncolytic vaccinia virus in cell cultures prognosticates the virulence and antitumor efficacy in mice. *J Transl Med* **9**: 164.
- Weibel, S, Raab, V, Yu, YA, Worschech, A, Wang, E, Marincola, FM *et al.* (2011). Viral-mediated oncolysis is the most critical factor in the late-phase of the tumor regression process upon vaccinia virus infection. *BMC Cancer* **11**: 68.
- Kirn, DH and Thorne, SH (2009). Targeted and armed oncolytic poxviruses: a novel multi-mechanistic therapeutic class for cancer. *Nat Rev Cancer* **9**: 64–71.
- Tóvári, J, Gilly, R, Rásó, E, Paku, S, Bereczky, B, Varga, N *et al.* (2005). Recombinant human erythropoietin alpha targets intratumoral blood vessels, improving chemotherapy in human xenograft models. *Cancer Res* **65**: 7186–7193.
- Katz, O, Gil, L, Lifshitz, L, Prutchi-Sagiv, S, Gassmann, M, Mittelman, M *et al.* (2007). Erythropoietin enhances immune responses in mice. *Eur J Immunol* **37**: 1584–1593.
- Prutchi-Sagiv, S, Golishevsky, N, Oster, HS, Katz, O, Cohen, A, Naparstek, E *et al.* (2006). Erythropoietin treatment in advanced multiple myeloma is associated with improved immunological functions: could it be beneficial in early disease? *Br J Haematol* **135**: 660–672.
- Rocchetta, F, Solini, S, Mister, M, Mele, C, Cassis, P, Noris, M *et al.* (2011). Erythropoietin enhances immunostimulatory properties of immature dendritic cells. *Clin Exp Immunol* **165**: 202–210.
- Mittelman, M, Neumann, D, Peled, A, Kanter, P and Haran-Ghera, N (2001). Erythropoietin induces tumor regression and antitumor immune responses in murine myeloma models. *Proc Natl Acad Sci USA* **98**: 5181–5186.



35. Hicks, AM, Riedlinger, G, Willingham, MC, Alexander-Miller, MA, Von Kap-Herr, C, Pettenati, MJ *et al.* (2006). Transferable anticancer innate immunity in spontaneous regression/complete resistance mice. *Proc Natl Acad Sci USA* **103**: 7753–7758.
36. Engert, A (2005). Recombinant human erythropoietin in oncology: current status and further developments. *Ann Oncol* **16**: 1584–1595.
37. Ludwig, H, Van Belle, S, Barrett-Lee, P, Birgegård, G, Bokemeyer, C, Gascón, P *et al.* (2004). The European Cancer Anaemia Survey (ECAS): a large, multinational, prospective survey defining the prevalence, incidence, and treatment of anaemia in cancer patients. *Eur J Cancer* **40**: 2293–2306.
38. Ribatti, D, Presta, M, Vacca, A, Ria, R, Giuliani, R, Dell’Era, P *et al.* (1999). Human erythropoietin induces a pro-angiogenic phenotype in cultured endothelial cells and stimulates neovascularization *in vivo*. *Blood* **93**: 2627–2636.
39. Doleschel, D, Mundigl, O, Wessner, A, Gremse, F, Bachmann, J, Rodriguez, A *et al.* (2012). Targeted near-infrared imaging of the erythropoietin receptor in human lung cancer xenografts. *J Nucl Med* **53**: 304–311.
40. Kumar, SM, Yu, H, Fong, D, Acs, G and Xu, X (2006). Erythropoietin activates the phosphoinositide 3-kinase/Akt pathway in human melanoma cells. *Melanoma Res* **16**: 275–283.
41. Mohyeldin, A, Lu, H, Dalgard, C, Lai, SY, Cohen, N, Acs, G *et al.* (2005). Erythropoietin signaling promotes invasiveness of human head and neck squamous cell carcinoma. *Neoplasia* **7**: 537–543.
42. Lai, SY, Childs, EE, Xi, S, Coppelli, FM, Gooding, WE, Wells, A *et al.* (2005). Erythropoietin-mediated activation of JAK-STAT signaling contributes to cellular invasion in head and neck squamous cell carcinoma. *Oncogene* **24**: 4442–4449.
43. Falkner, FG and Moss, B (1990). Transient dominant selection of recombinant vaccinia viruses. *J Virol* **64**: 3108–3111.